Bioscience of Microbiota, Food and Health Vol. 44 (2), 146–159, 2025

Full Paper

Correlation between differences in the intestinal flora structure and Chinese medicine evidence in patients with Wilson disease-related liver fibrosis analyzed via high-throughput sequencing technology

Yue PU[1], Xinxiang ZHANG[2], Juan ZHANG[1*], Daojun XIE[1], Han WANG[1], Hong CHEN[1], Ying MA[1], Nian PENG[1], Rui LI[1] and Hao YE[1]

[1]*The First Affiliated Hospital of Anhui University of Chinese Medicine, Hefei, Anhui, China*
[2]*Lu'an People's Hospital of Anhui Province, Lu'an, Anhui, China*

Received August 3, 2024; Accepted November 23, 2024; Published online in J-STAGE December 11, 2024

To observe the composition and abundance of the intestinal flora in patients with Wilson disease (WD)-related liver fibrosis and analyze the correlation between the composition of intestinal flora of patients and the evolution of evidence from Chinese medicine, we selected 237 patients with WD-related liver fibrosis and 30 healthy volunteers from the Brain Disease Center of Anhui Provincial Hospital of Chinese Medicine. The patients with WD-related liver fibrosis were divided into 5 groups according to traditional Chinese medicine (TCM) evidence (dampness-heat syndrome, group A; intermingled phlegm and blood stasis syndrome, group B; liver wind stirring up internally syndrome, group C; yin deficiency of the liver and kidney syndrome, group D; and yang deficiency of the spleen and kidney syndrome, group E) and a group healthy volunteers (group F), which served as the control. Stool samples were obtained from the patients in the 6 groups. The 16S rRNA sequencing technique was used to analyze the intestinal flora of the different TCM evidence groups of WD patients and the healthy control group and subjected to a statistical analysis. The intestinal flora abundance was significantly lower in patients with WD-related liver fibrosis than in healthy controls, and the decrease in strain content was more significant in patients with deficiency evidence in groups D and E. In terms of the structure of the phylum-level flora, the Firmicutes phylum was still the dominant phylum, but the contents of the evidence-type groups all decreased, with the most obvious decreases in groups D and E. The results for the Actinobacteria phylum were similar, whereas the opposite was true for the Proteobacteria phylum. The section-level and genus-level results corresponded to the gate level. The intestinal flora of the WD-related liver fibrosis patients and healthy controls differed in terms of abundance and intestinal flora structure, and there were also differences between different Chinese medicine certificates.

Key words: Wilson disease, intestinal flora, Chinese medicine evidence, correlation

INTRODUCTION

Hepatolenticular degeneration (HLD), also known as Wilson's disease (WD), is an autosomal recessive disorder caused by mutations in the ATP7B gene encoding the ATP7B copper transport protein [1]. Mutations in this gene lead to reduced synthesis of copper cyanoproteins, causing a large accumulation of copper ions in the body, which affects mainly the liver and brain [2]. Eventually, patients may develop a variety of clinical manifestations, such as hepatic fibrosis leading to cirrhosis and damage to the basal ganglia region [3, 4]. The clinical manifestations of the disease are complex and varied, but hepatic fibrosis is the main pathological change in the liver of nearly every patient with WD, regardless of whether the condition is hepatic, cerebral, or another type [5]. Hepatic fibrosis is an early stage of end-stage liver disease and is a reversible process [6]. Numerous studies have shown that early and effective treatment can reverse liver fibrosis and significantly control disease progression to reduce mortality [7, 8].

The root cause of WD-related liver fibrosis is copper metabolism due to mutations in the ATP gene, which results in the deposition of large amounts of copper ions in the liver,

*Corresponding author. Juan Zhang (E-mail: 1477210980@qq.com)

doi: 10.12938/bmfh.2024-081

leading to mitochondrial dysfunction, lipid peroxidation, oxidative stress, something like and other, inducing intracellular inflammatory storms and the secretion of a variety of cytokines [9]. These cytokines can stimulate hepatic stellate cells to become myofibroblasts, and massive proliferation, accumulation, and imbalance of degradation lead to excessive deposition of extracellular matrix, abnormalities in the liver tissue structure, and eventual formation of hepatic fibrosis [10]. During ongoing liver damage, the functions of the liver, such as synthesizing albumin, are weakened, the synthesis of body substances is slowed, and the process of self-repair is slowed. The mesentery is more sensitive to hypoxia or ischemia due to the "lack of raw materials" and is prone to necrosis and detachment, thus increasing the permeability of the intestinal wall and making it easier for endotoxins and other toxins to flow into the body [11]. Therefore, the diversity of the intestinal flora varies at different stages of liver disease and is inextricably linked to systemic inflammation. When inflammation occurs in the liver, there is an imbalance in bile acid secretion, and either a lack of bile acids in the gut or an accumulation of bile acids in the gut may lead to overgrowth of bacteria and potent pathogens, which can exacerbate the risk of inflammation, bacterial translocation, hydrophobicity, and ionic transmembrane flow [12]. In addition, an imbalance in bile acid secretion affects the integrity of the intestinal epithelium and the mucosal immune response, thus indirectly regulating the composition of the microbial community [13]. A recent animal study revealed that hepatocellular carcinoma (HCC) mice induced with streptozotocin presented a significant increase in hydrophobic bile acids in the liver, downregulation of genes involved in bile acid synthesis and transport (e.g., CYP7A1 and BSEP), and a consequent change in the intestinal flora as they progressed from liver fibrosis to hepatocellular carcinoma [14]. The researchers further reported increasing levels of *Enterobacteriaceae* and *Clostridia* and a gradual decrease in the abundance of *Lachnospiraceae* in the gut flora structure of the mice. Another study revealed that feeding secondary bile acids or colonization with bile acid-metabolizing bacteria regulated the structure of the intestinal flora in mice, protected the integrity of the intestinal mucosa, reduced the level of the inflammatory cytokine IL-6, and restored intestinal homeostasis to resist hepatic inflammation, thereby reversing hepatic fibrosis [15].

The intestinal tract is not only an important organ for the digestion and absorption of nutrients in the human body but also the first line of immune defense against food-derived antigens and pathogenic microorganisms. The human gut microbiota contains more than 3 million genes from bacteria, fungi, and viruses with high metabolic capacity [16], and its metabolites can act as important signaling molecules to the liver, which in turn can reflexively signal to the gut. This loop of intercommunication between the gut and the liver is known as the gut–liver axis [17]. The gut–liver axis is the result of a close interaction between the anatomy and physiology of the gastrointestinal tract and the liver, which is mediated mainly by the portal circulation [18]. The close relationship between the gut and the liver underlies the regulatory role of the gut microbiota in liver health [19]. Recent studies have revealed a significant reduction in the abundance and diversity of gut microorganisms in patients with liver fibrosis, with a decrease in beneficial bacteria and an increase in potentially pathogenic bacteria [20]. In addition, the gut microbiota influences the progression of hepatic fibrosis, mainly by maintaining gut barrier function and regulating metabolic function and the immune system [21]. Most of the current studies have been conducted only on patients with simple liver fibrosis, while the structure of the intestinal flora in patients with WD-related liver fibrosis has been less studied.

Patients with WD-related liver fibrosis have a wide range of clinical manifestations, including yellowing of the body and eyes, plumpness and dullness, and distension of the stomach and abdomen. Therefore, the symptoms can be summarized into the categories of "distention and fullness", "jaundice", and "distention" in Chinese medicine. The Chinese medical etiology of this disease primarily stems from a lack of innate endowment and an uncontrolled diet, resulting in the accumulation of copper toxin, stagnation of qi, and accumulation of phlegm and dampness, which eventually transform into heat. This heat generates wind, causing the liver wind to move inward. The disease is prolonged and affects the kidneys, resulting in deficiency of the liver and kidneys, which ultimately damages the spleen and stomach and leads to dysfunction of the spleen and stomach and deficiency of yang qi in the spleen and kidneys [22]. Therefore, according to the clinical manifestations and signs of WD patients and previous relevant studies, the different stages of the disease can be dialectically categorized into five types: internal dampness-heat, phlegm-blood stasis, internal movement of the liver wind, deficiency of the liver and kidney, and deficiency of the spleen and kidney yang [23]. Chinese medicine evidence is a pathological generalization of a certain stage in the process of disease occurrence and development, with dynamic and immediate characteristics. At this stage, the use of biological methods to find the objective basis of traditional Chinese medicine (TCM) symptoms has become a research hotspot in the field of TCM, with the goal of revealing the nature of symptoms from an objective point of view. Therefore, this study explored the correlation between the bacterial flora structure of WD patients and the two dynamic change mechanisms of Chinese medicine patterns from the perspective of the intestinal flora and explored whether bacterial flora characteristics may be the microcosmic embodiment of Chinese medicine patterns to provide new ideas and research directions for the early detection and treatment of different patterns of WD.

MATERIALS AND METHODS

Source of cases

We screened patients with WD with liver fibrosis who were diagnosed from December 2021 to December 2023 at the First Affiliated Hospital of Anhui University of Traditional Chinese Medicine. Each diagnostic criterion, inclusion criterion, and exclusion criterion was strictly evaluated. A total of 237 patients with five types of evidence of WD-related liver fibrosis were included, and 30 healthy volunteers composed the control group.

Diagnostic standards

The diagnostic criteria for WD referred to the Chinese Guidelines for the Diagnosis and Treatment of Hepatobiliary Nuclear Degeneration 2021 developed by the Chinese Medical Association [24]. For the diagnosis of liver fibrosis, reference was made to the Guidelines for Integrated Chinese and Western Medicine Diagnosis and Treatment of Liver Fibrosis (2019 edition) written by the Liver Disease Committee of the Chinese

doi: 10.12938/bmfh.2024-081

Society of Integrative Medicine [25]. TCM identification and typing were developed with reference to the WD Integrated Chinese and Western Medicine Treatment Guidelines 2021 [26].

Inclusion and exclusion criteria

The inclusion criteria for patients were as follows: (1) met the diagnostic criteria for WD, (2) met the diagnostic criteria for hepatic fibrosis, and (3) classified according to the above diagnostic criteria by TCM.

The exclusion criteria were as follows: (1) age <10 years or >50 years; (2) pregnant or lactating woman; (3) severe mental behavioral abnormalities; (4) viral hepatitis, autoimmune hepatitis, or alcoholic liver disease; (5) patient with a severe condition, such as hepatic encephalopathy, hepatorenal syndrome, upper gastrointestinal tract hemorrhage, or portal vein thrombosis, or other unstable patient; and (6) asymptomatic patient with WD.

Sample collection and preservation

Fresh feces excreted early in the morning by members of the WD liver fibrosis group and the healthy volunteer group were collected. To avoid contamination of the samples, urine was emptied beforehand, and all members defecated in a relatively sterile area to avoid other factors influencing the results of the study. The patient defecated into a preprepared container, and an uncontaminated portion (approximately 5 g) was selected via a sterile stool picker and sealed in a sterile environment. We then numbered the samples and stored them at −80°C for further analysis.

DNA extraction of the fecal flora

After all our samples from the WD liver fibrosis patients and healthy volunteers were collected, a DNA extraction kit was used to extract the total DNA from the samples. The NanoDrop technique was applied to quantify the DNA of the samples, and the quality of the extracted DNA was analyzed via the 1.2% agarose gel electrophoresis detection technique.

Polymerase chain reaction (PCR) amplification

During the PCR amplification process, the number of cycles of amplification was highly controlled, and the number of recirculations was minimized, while the amplification conditions were the same for all samples. When amplification was performed, a negative control group was set up so that microbial contamination of the environment and reagents could be detected and the rigor of the experiment could be ensured.

Purification and recovery of amplification products by magnetic beads

Vazyme VAHTS^{TM} DNA Clean Beads (beads:product=0.8:1; Nanjing Vazyme Biotechnology Co., Ltd., Nanjing, China) were added to 25 μL of PCR product, mixed thoroughly, placed on a magnetic rack, and allowed to adsorb for 5 min, and then the supernatant was removed. Then, 20 μL of 0.8-fold magnetic bead wash solution was added, mixed thoroughly, placed on a magnetic rack, and allowed to adsorb for 5 min, and then the supernatant was removed. Two hundred microliters of 80% ethanol was added, and the mixture was placed in the opposite direction on the magnetic stand. The supernatant was removed after 30 sec, after which the mixture was incubated at room temperature for 5 sec. When the ethanol volatilized, cracks were observed in the magnetic beads, indicating process completion. A total of 25 μL of elution buffer (Takara Biomedical Technology (Beijing) Co., Ltd., Beijing, China) was added for elution, and the PCR tube (Axygen Scientific, Inc., San Jose, CA, USA) was placed in an adsorption rack and left there for 5 min. Once fully adsorbed, the supernatant was removed, and the mixture was sealed. On the basis of the fluorescence quantification results, each sample was mixed in the appropriate proportion according to the sequencing volume required for the sample.

Sequencing library preparation

End Repair Mix 2 (Thermo Fisher Scientific, Waltham, MA, USA) was used to excise the protruding base at the 5 end of the DNA sequence, and during the excision process, a phosphate group was added to complement the missing base at the 3 end. To avoid self-attachment of the DNA fragments and ensure that the target sequence can be connected to the sequencing junction smoothly, the DNA sequence needs to be modified by adding an A base at the 3 end. To ensure that the DNA molecule is firmly placed on the Flow Cell (Takara Biomedical Technology (Beijing) Co., Ltd.), it is necessary to add the appropriate sequencing street to the 5 end of the DNA sequence, i.e., the sequencing junction possessed by the library-specific tag (index sequence). We used Beckman AMPure XP Beads (Axygen Scientific, Inc., San Jose, CA, USA) to remove the junction self-associated fragments via magnetic bead screening and purify the library system after junction addition. The above treated DNA fragments were amplified via PCR and the library enrichment products were purified again via Beckman AMPure XP Beads (Axygen Scientific, Inc.). Finally, 2% agarose gel electrophoresis was used to finalize the sequencing library.

Statistical methods

All the data in this study were statistically analyzed using the IBM SPSS Statistics 26.0 statistical software, and one-way ANOVA was used for samples from multiple groups that simultaneously satisfied normality, χ^2 tests of variance, and independence. The Kruskal–Wallis H rank sum test was used if the above application conditions were not met. Completely randomized unordered categorical variable information for correlation and difference analysis was analyses via the χ^2 tests. Differences were statistically significant at $p<0.05$ and significant at $p<0.01$.

Ethics

This study was reviewed and approved by the Ethics Committee of the First Affiliated Hospital of Anhui University of Traditional Chinese Medicine (Grant No. 2022MCZQ18).

RESULTS

Analysis of general clinical data

A total of 237 patients with WD-related liver fibrosis and 30 normal healthy individuals were included. After dialectical typing, the included patients were divided into five groups: damp-heat internalization syndrome group (A), phlegm-stasis interconjunction syndrome group (B), liver-wind internalization syndrome group (C), liver-kidney deficiency syndrome group (D), and spleen-kidney yang deficiency syndrome group (E). There were no significant differences in sex, age, or degree of disease

Table 1. General information analysis

Features	Numbers	Age (years)	Gender (male)	Duration of disease (years)
Group A	50	28.54 ± 6.27	27 (54.0%)	7.32 ± 3.09
Group B	60	29.33 ± 4.77	26 (43.3%)	7.17 ± 2.79
Group C	44	27.70 ± 5.45	20 (45.5%)	6.80 ± 3.28
Group D	43	29.28 ± 6.52	21 (48.8%)	6.77 ± 3.29
Group E	40	26.83 ± 6.63	23 (57.5%)	6.89 ± 3.96
Group F	30	30.40 ± 5.97	16 (53.3%)	6.90 ± 3.23
F/χ^2	-	1.767	2.803	0.253
p-value	-	0.120	0.730	0.908

among the six groups (including the control group; p>0.05), and the study data were comparable (Table 1).

Annotated statistics on operational taxonomic unit (OTU) classification of intestinal flora

Using the R package VennDiagram (v1.6.20) software, the valid tags obtained from the Quality Control were classified into OTUs according to 97% similarity, and the similarity and specificity of the composition of the OTUs in the environmental samples could be visualized through a Venn diagram, as shown in Fig. 1. The six groups contained 85 shared OTUs, as well as 576 OTUs specific to group A (damp-heat internalization syndrome), 274 OTUs specific to group B (phlegm-stasis mutual conjugation syndrome), 96 OTUs specific to group C (liver-qi stagnation syndrome), 111 OTUs specific to group D (liver-kidney-yin dystrophy syndrome), 12 OTUs specific to group E (spleen-kidney-yang deficiency syndrome), and 444 OTUs specific to group F (healthy control). Sample richness information in the OTUs provides an initial indication of the species richness of a sample.

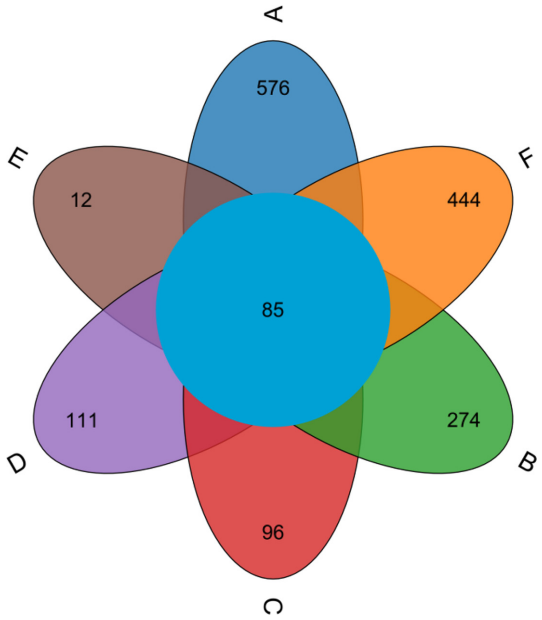

Fig. 1. The operational taxonomic unit (OTU)/ amplicon sequence variant (ASV) distribution Venn diagram presents the number of species in the six sets of samples in different colors, with overlapping areas representing the number of shared species.

Species richness alpha diversity analysis

Alpha diversity analysis can be used to measure species richness in community ecology and is a composite indicator of species richness and evenness. In this study, rarefaction, rank-abundance, and species accumulation curves were used to analyze the species diversity and abundance of the intestinal flora in the samples, all of which were part of the alpha diversity analysis.

Species richness dilution curve analysis

The shape of a rarefaction curve can directly reflect the reasonableness of the amount of test data and indirectly reflect the abundance of species in samples, as shown in Fig. 2. As the number of sequences increases, the curve gradually flattens out. When the species accumulation curve flattens, it indicates that the amount of sequencing data is asymptotically reasonable and that more data will produce only a very small number of new species (OTUs). According to Fig. 2, the sample sequence data measured in this experiment were sufficient and reasonable.

Species richness rank-abundance curves

The rank-abundance curve is a graph constructed on the basis of the number of sequences belonging to OTUs in the relevant samples, with the OTUs as the horizontal coordinate (ranked according to abundance) and their corresponding number of sequences (i.e., abundance) as the vertical coordinate. As shown in Fig. 3, the species richness of the samples from group F (control) was the highest, meaning that the species richness was lower for the five evidence groups. Among the five evidence groups, species richness was significantly lower in groups D and E than in the other groups, and that of group E was the lowest.

Intestinal flora species accumulation curve

As shown in Fig. 4, the curve sharply increases when the sample size does not reach 20, and the curve gradually flattens out after the sample size exceeds 20. As the sample size increases, the species no longer significantly increase, again indicating adequate sampling.

Analysis of differences in the diversity index of intestinal flora

A boxplot comparing the differences in flora among groups A, B, C, D, E, and F, based on the Chao1, Shannon, and Simpson indices is shown in Fig. 5. The Chao1 index indicates the number of OTUs contained, so larger values indicate more species contained in a sample. The Chao1 index was significantly reduced in the 5 evidence type groups compared with the control group (p<0.001). Moreover, as the evidence type of

doi: 10.12938/bmfh.2024-081

WD patients shifted from solid to deficient, the Chao1 index of the species also gradually decreased, as shown in Fig. 5A. The Shannon index can be used to assess the richness and evenness of species composition in a sample. Larger values indicate that the environment is more species-rich and more evenly distributed across species. The Shannon index statistics were similar to those of the Chao1 index, with significant differences between the 5 evidence groups and the control group ($p<0.001$). Furthermore, the bacterial abundance showed a more pronounced decrease in group E ($p<0.001$), as shown in Fig. 5B. Simpson's index is the probability that two OTUs randomly selected from sample data belong to different species. Therefore, Simpson's index is different from the above two indices, which are inversely proportional to community diversity (Fig. 5C).

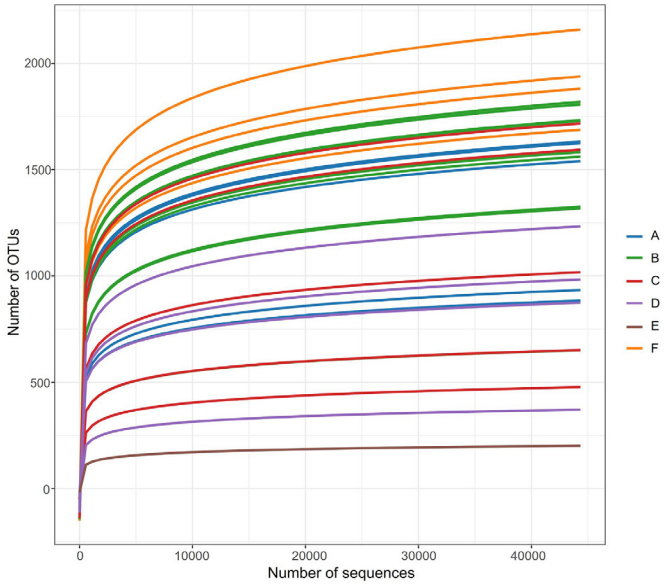

Fig. 2. The six groups of data are represented by different colors in the rarefaction curve. The horizontal coordinate is the amount of sequencing data extracted, and the vertical coordinate is the number of operational taxonomic units (OTUs).

Principal component analysis of bacterial colonies

The similarity of sample compositions can be reflected in a principal component analysis (PCA) plot. The higher the similarity in sample composition, the more concentrated the points are in the plot; conversely, the more dispersed the distribution, the lower the similarity. As shown in Fig. 6, among all the main coordinate components, the one that showed the most variability was the horizontal coordinate PC2 (with an explanation degree of 28.397%). The PCA shows that the samples of each evidence type group (A, B, C, D, and E) were distributed farther from group F on PC2 and that the distribution distances of groups A, B, and C were close to each other. We then further analyzed the gut microbes between the groups via supervised PLS-DA discriminant analysis, and as shown in Fig. 7, groups D and E were significantly clustered. On the other hand, the five evidence groups were significantly dispersed compared with the control group (group F). The above results suggest that the structural composition of the gut microorganisms was similar in patients in groups D and E, with differences between groups A, B, and C. Additionally, the compositions of the gut microorganisms in the five evidence groups were significantly different from that in group F.

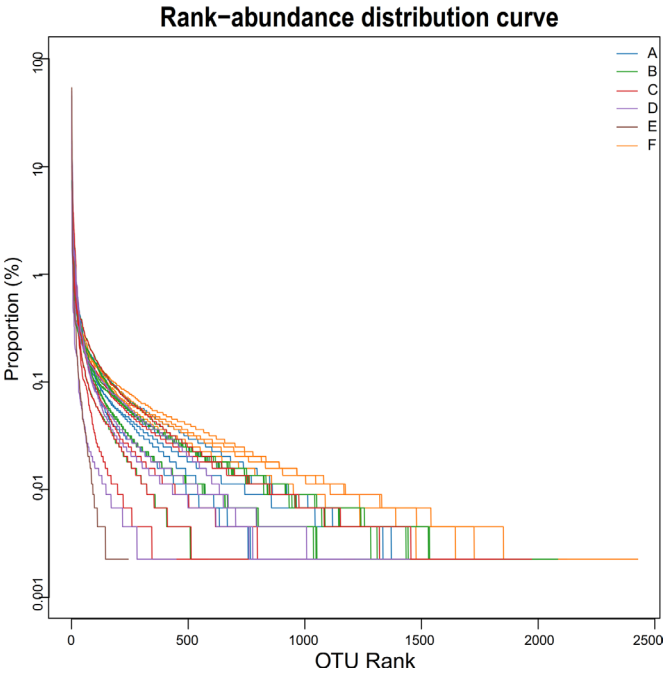

Fig. 3. Species richness rank-abundance curves were plotted for each sample by counting the number of corresponding operational taxonomic unit (OTU) sequences and then plotting them in ascending order according to the number of sequences.

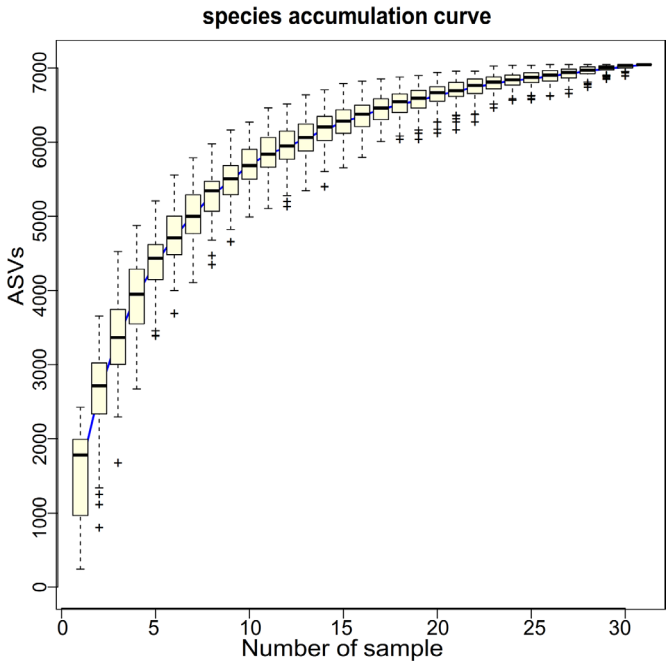

Fig. 4. Species accumulation curve presents the total number of operational taxonomic units (OTUs)/ amplicon sequence variants (ASVs) included in the sample as the number of random samples increases.

doi: 10.12938/bmfh.2024-081

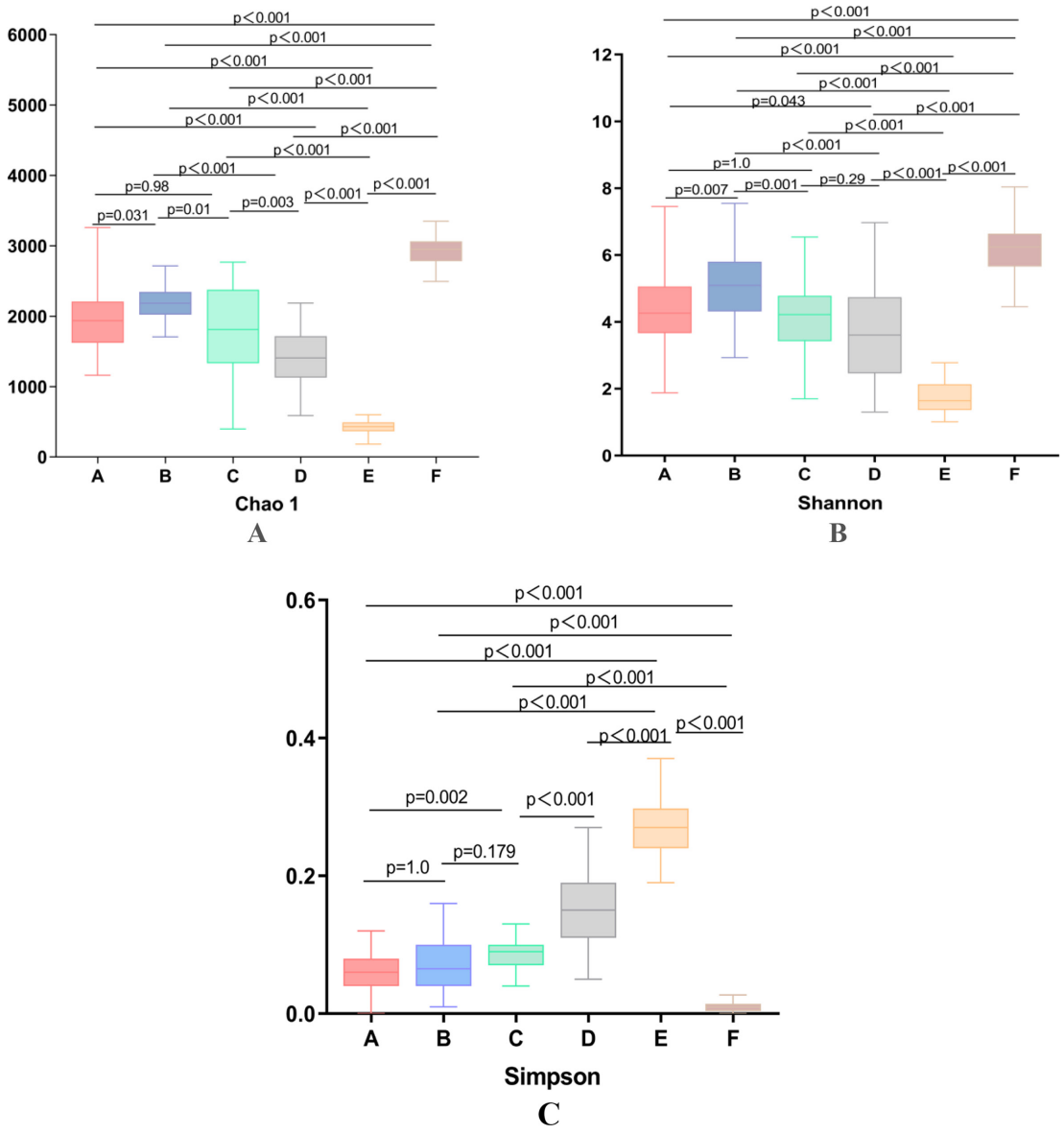

Fig. 5. Diversity index boxplots in which A, B, and C refer to the intestinal flora Chao1, Shannon, and Simpson index statistic boxplots of the six groups, respectively. The two groups corresponding to the start and end of the horizontal line directly below the top of each boxplot were statistically analyzed to derive p-values and labeled.

Heatmap of flora classification

The analytes in this study consisted of taxonomic units at the genus level for each group of subjects, and the top 100 genera in terms of relative abundance were plotted on a heatmap of genus richness, with the colors in the map representing the magnitude of abundance of the species. The color box at the bottom of Fig. 8 shows the corresponding percentage of species abundance as a gradient from blue to red. The colony clustering diagram allows for the differentiation of taxonomic units of high and low abundance, with color gradients and degrees of similarity reflecting similarities and differences in the composition of multiple samples at each taxonomic level. The heatmap shows the species composition of each sample. The more similar the species are in the left side of the figure, the closer they are in the clustering tree. Furthermore, the closer the distance is in the clustering tree, the shorter the branching distance of the clusters. This can reflect the similarity and difference in species composition for all the samples at a particular taxonomic level. As shown in Fig. 8, at the genus level, the most abundant genera of bacteria in patients with the damp-heat internalization syndrome, phlegm-stasis mutual conjugation syndrome, and liver-wind internalization syndrome were *Escherichia* and *Unassigned*, and the genera with the highest abundances in the patients with liver-kidney deficiency syndrome and spleen-kidney yang-deficiency syndrome were *Escherichia* and *Megamonas*. The most abundant genera in the evidence groups showed extremely low abundances in the control group, with *Bifidobacterium* and *Faecalibacterium* being the most abundant genera in the control group.

doi: 10.12938/bmfh.2024-081

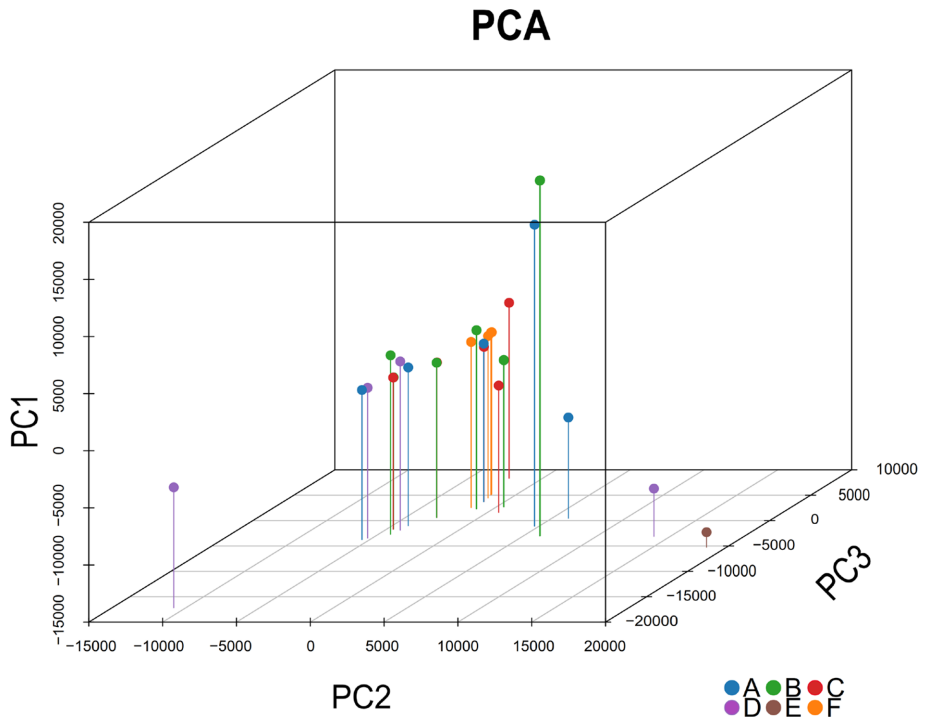

Fig. 6. Each point in the principal component analysis plot represents a sample, and the different colors of the points indicate the subgroups to which the samples belong. A closer distribution of the points indicates that the samples are more similar.

Distribution and differences in the bacterial flora structure at the portal level

Comparative observations of the composition and relative abundance of the microflora among the six groups revealed a high degree of variability in the number of major phyla between the evidence groups of patients with WD-related liver fibrosis and the control group (group F). The dominant phylum in all six groups of samples was still *Firmicutes*, but its level was lower in all groups with WD-related liver fibrosis than in group F; the opposite was true for *Proteobacteria*. All five evidence groups also presented lower levels of the *Actinobacteria* phylum than the control group (group F). The most significant decrease in the abundance of the *Bacteroidetes* phylum ($p<0.05$) and the highest percentage of the *Proteobacteria* phylum ($p<0.05$) were observed in group E, as shown in Fig. 9A and 9B.

Distribution of and differences in bacterial flora structure at the family level

The dominant flora at the family level for the six groups of samples were *Lachnospiraceae*, *Enterobacteriaceae*, *Bifidobacteriaceae*, *Rumatobacteriaceae*, and *Bacteroidaceae*. At the family level, *Selenomonadaceae* and *Enterobacteriaceae* showed the highest abundances in group E and were significantly greater than those in group F ($p<0.05$). The species richness of *Bifidobacteriaceae* was significantly reduced in the five evidence groups, with the most pronounced reduction in group E. The abundance of *Lachnospiraceae* in the control group (group F) was significantly greater than those in the five evidence groups, with the lowest content observed in group E. The differences were statistically significant ($p<0.05$; Fig. 10).

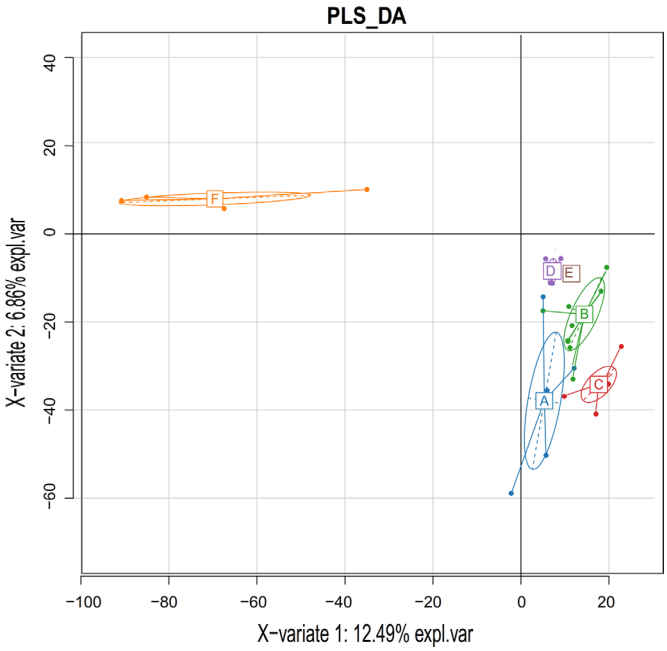

Fig. 7. Points of different colors or shapes in the partial least squares discriminant analysis plot represent sample groups in different environments or conditions, and the scales of the horizontal and vertical axes are relative distances.

Distribution of and differences in bacterial flora structure at the genus level

The dominant genera at the genus level were *Bifidobacterium*, *Escherichia*, *Faecalibacterium*, and *Megamonas*. The five

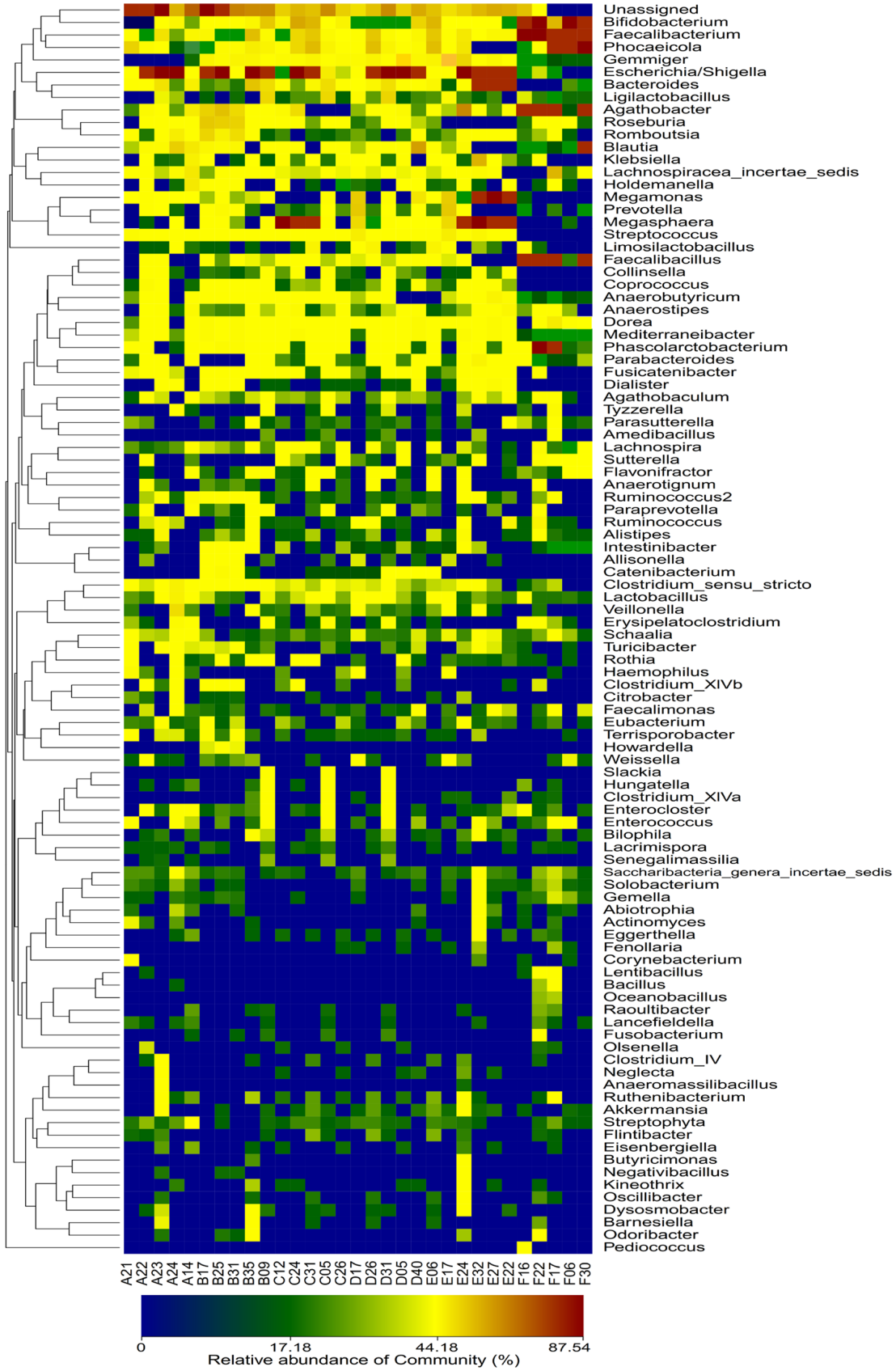

Fig. 8. The heatmap of the flora classification presents the 100 most abundant species detected in a randomly selected sample. The colors in the graph represent the magnitude of the abundance of the species, with the gradient from blue to red indicating low to high species abundance.

doi: 10.12938/bmfh.2024-081

evidence groups presented significantly lower *Bifidobacterium* abundances than the control group (group F), with the most significant decrease observed in group E ($p<0.05$). The levels of *Escherichia* in the bacterial flora of the five evidence groups were significantly greater than those of the control group, with the increases being more pronounced in groups B, D, and E. In addition, the levels of *Faecalibacterium* were all lower in the evidence groups than in the control group, with more significant decreases observed in groups C, D, and E, as shown in Fig. 11A and 11B.

DISCUSSION

In this study, we analyzed the composition and structure of the intestinal flora in stool samples from different evidence groups of patients with WD-related liver fibrosis via high-throughput sequencing of the V3–V4 region of 16S RNA and compared the results with those of a healthy control group (group F). First, after alpha diversity analysis, the sample size selected for this experiment was sufficient, and the data were real and reasonable, which confirmed the differences between the five common types of evidence in WD patients and the healthy control group. We

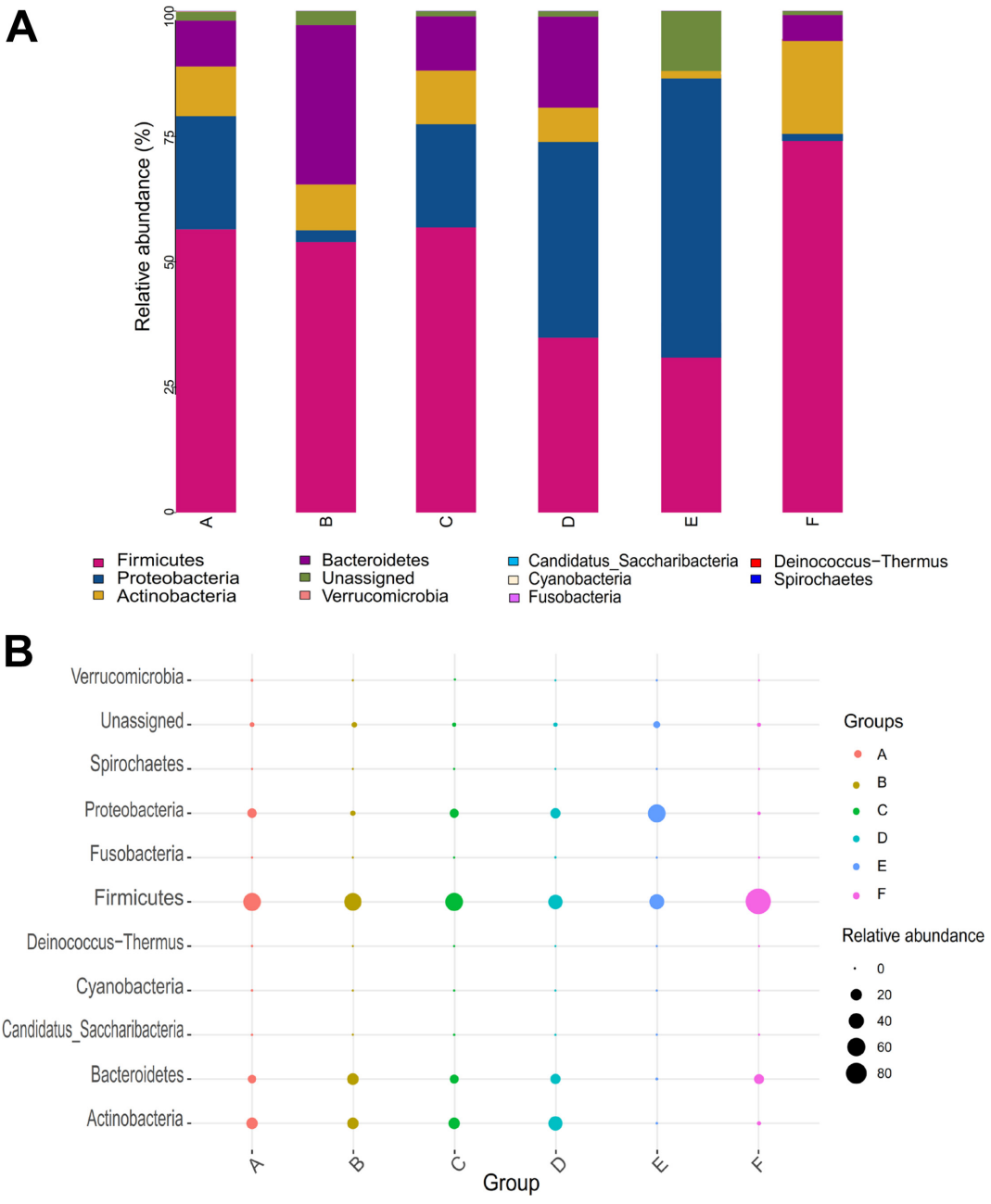

Fig. 9. A. Histogram of species composition at the phylum level for each group of mycobacteria. Each color in the diagram corresponds to one species, and the corresponding species are shown in the color annotations at the bottom of the histogram. B. Bubble diagram of the distribution of species abundance at the phylum level for each group of bacteriophages, with the size of the dots indicating the relative abundance of the species in the sample and the different colors of the dots indicating the different sample groups.

doi: 10.12938/bmfh.2024-081

compared the differences in the flora counts of the six groups in terms of the Chao1, Shannon, and Simpson indices. The results revealed that the intestinal flora counts of the WD patients with liver fibrosis were significantly lower than those of the healthy control group, and the differences were statistically significant ($p<0.05$). Moreover, as the patients' conditions progressed, the evidence pattern changed from solid to deficient, from the beginning of damp-heat internalization, phlegm-stasis mutual conjugation, and hepatic wind internalization to evidence of liver-kidney deficiency and spleen-kidney yang deficiency, and the

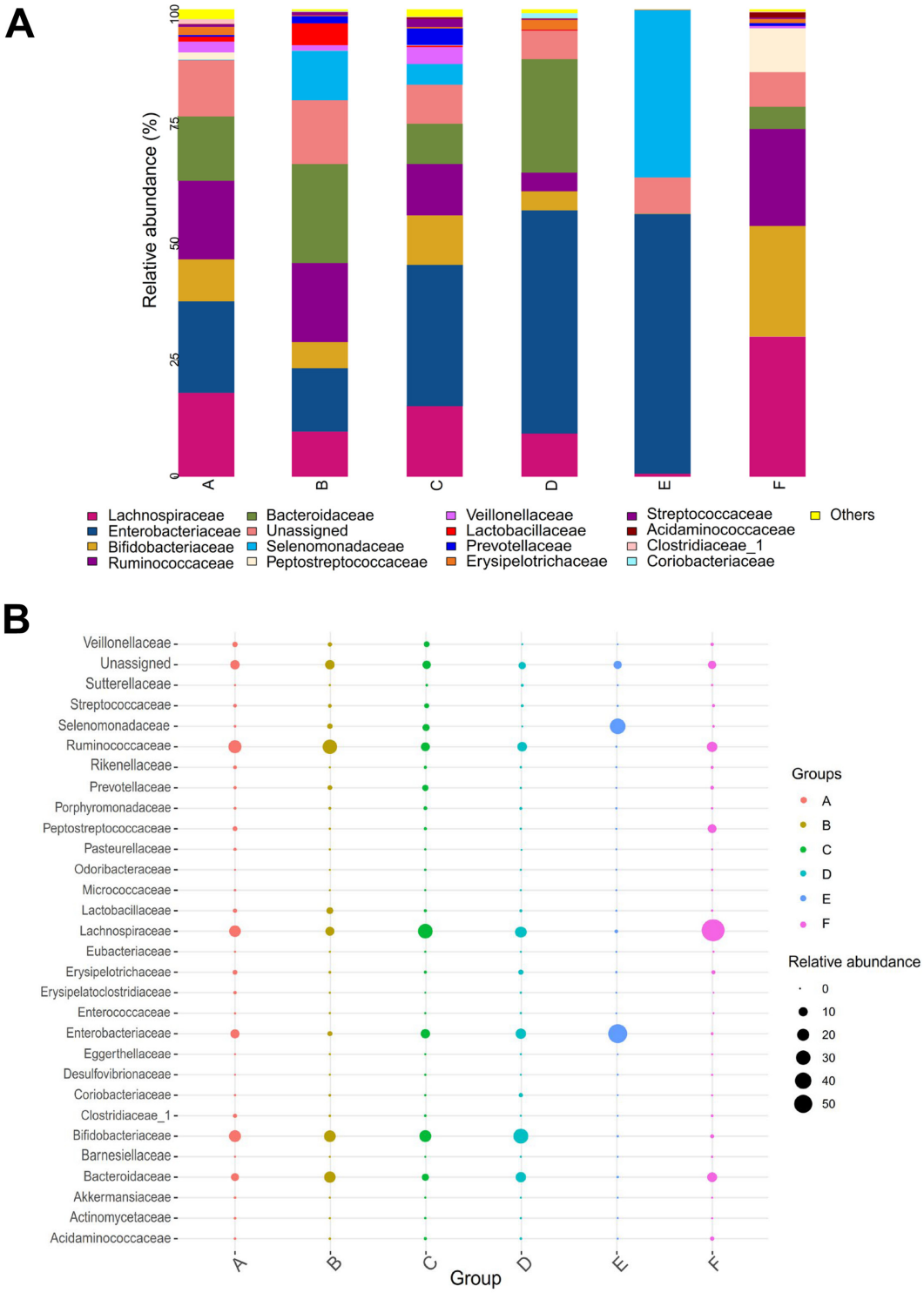

Fig. 10. A. Histogram of species composition at the family level for each group of mycobacteria. Each color in the diagram corresponds to one species, and the corresponding species are shown in the color annotations at the bottom of the histogram. B. Bubble diagram of the distribution of species abundance at the family level for each group of mycobacteria, with the size of the dots indicating the relative abundance of the species in the sample and the different colors of the dots indicating the different sample groups.

doi: 10.12938/bmfh.2024-081

intestinal flora richness in the body was also gradually decreased. PCA and PLS-DA of the principal components revealed that the gut microbial compositions of the evidence groups were significantly different from that of the control group. There were also significant differences between groups A, B, and C, while the microbial structural composition was similar in Groups D and E. The microbial compositions of the evidence groups were significantly different from that of the control group. The heatmap

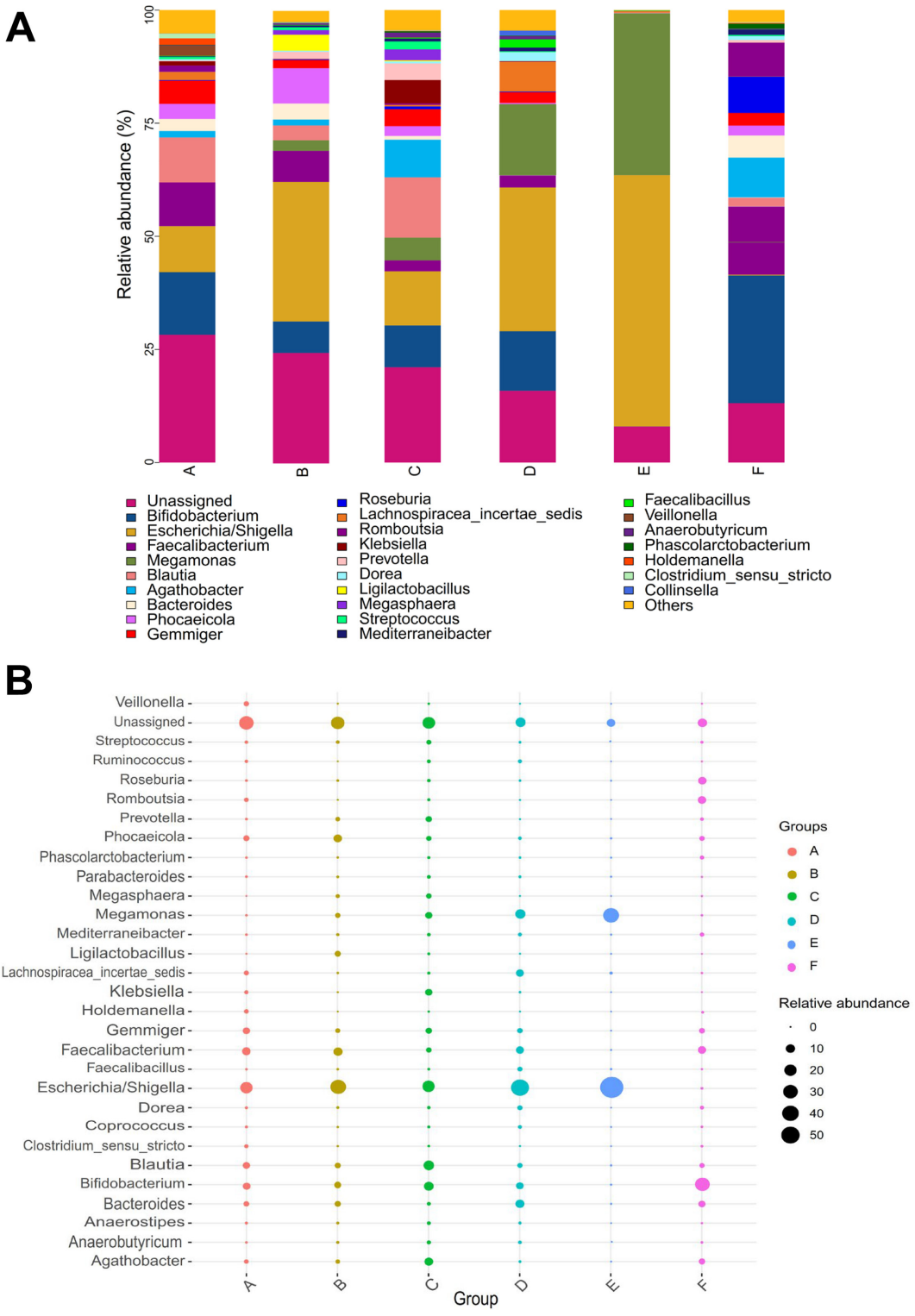

Fig. 11. A. Histogram of species composition at the genus level for each group of mycobacteria. Each color in the diagram corresponds to one species, and the corresponding species are shown in the color annotations below the histogram. B. Bubble diagram of the distribution of species abundance at the genus level for each group of mycobacteria, with the size of the dots indicating the relative abundance of the species in the sample and the different colors of the dots indicating different sample groups.

doi: 10.12938/bmfh.2024-081

of the flora classification similarly confirmed these findings, with differences in the most highly abundant flora in groups A, B, and C for patients with solid evidence versus groups D and E for patients with deficient evidence and the abundance of flora in the evidence groups being the inverse of that in the control group.

Homeostasis of the gut–liver axis is essential for maintaining the integrity of the intestinal mucus barrier and the physiological composition of the gut microbiome. In patients with WD-related liver fibrosis, the intestinal mucosal barrier is disrupted, bile secretion is reduced, and the liver influences the amount and composition of the intestinal flora by regulating bile acid secretion and signaling pathways mediated by bile acids [27]. An increasing number of studies have shown that there is an important link between the biodiversity and metabolites of the intestinal flora and the enterohepatic axis. Intestinal commensal microorganisms, as important components of the enterohepatic axis, promote inflammatory responses and lead to the development of hepatic fibrosis through mechanisms such as increasing the host's energy intake, regulating the metabolism of choline and bile acids, and activating pattern recognition receptors. Additionally, these factors are causative of each other [28].

Our experiments on the distribution of the microbial structure of the samples and analysis of differences revealed that *Firmicutes* remained the dominant phylum in all the groups, but its abundance was significantly lower within the bacterial flora of the evidence groups of patients with WD. *Firmicutes* are a large group of bacteria that are mostly gram-positive and constitute the most common phylum of the intestinal microbiota; organisms in *Firmicutes* constitute an important part of the normal flora [29]. Most *Firmicutes* are capable of producing endospores that are highly dehydrated and can resist dehydration and even survive in extreme conditions [30]. Pathologically, a reduction in *Firmicutes* can induce hepatic steatosis and promote elevated levels of TNF-α mRNA, suggesting that the absence of *Firmicutes* may affect the immune system, leading to an abnormal hepatic inflammatory response [31] Chronic inflammation over time can stimulate excessive proliferation of hepatic connective tissues and contribute to the development of hepatic fibrosis.

The *Actinobacteria* phylum belongs to one of the four major phyla of the intestinal flora in the human body and plays a crucial role in the maintenance of intestinal microenvironmental homeostasis. The main anaerobic families in this phylum are *Bifidobacteria* and *Propionibacteria*, with many studies focusing on *Bifidobacteriaceae*, which are the most representative of the intestinal tract [32]. Bifidobacteria and lactobacilli are the two most common probiotics [33]. Bifidobacteria play a key role in the enterohepatic axis by inhibiting inflammation and oxidative stress and preventing hepatic lipid deposition [34, 35]. Experimental studies further revealed that supplementation with probiotics such as *Bifidobacterium* in rats improved liver pathology, restored intestinal barrier integrity, regulated and improved intestinal microbiota dysbiosis reduced serum inflammatory cytokines, and possibly reversed liver fibrosis [36]. Notably, the abundance of *Bifidobacteria* was highest in the healthy control group both at the family level and at the genus level, with a gradual decrease in abundance as the evidence shifted from solid to deficient and the conditions further aggravated. Moreover, these findings provide new ideas for the treatment of WD-related liver fibrosis, and in the clinic, supplementation with *Bifidobacterium bifidum* can be attempted to achieve a balance of intestinal microorganisms and maintain the stability of the gut–liver axis to improve the clinical symptoms of patients.

In addition, we found that the phylum *Proteobacteria* and its corresponding genera *Enterobacteriaceae* and *Escherichia coli* varied significantly among the groups. *Proteobacteria* door colonization leads to significantly lower levels of glycine in the intestine, blood, and cerebrospinal fluid. However, glycine reduces hepatic fibrosis by decreasing intestinal mucosal permeability leading to reduced endotoxin absorption and decreased levels of enteric-derived endotoxin [37]; therefore, elevated levels of it may accelerate the process of hepatic fibrosis. The phylum *Proteobacteria* is gram-negative and contains many pathogenic bacteria, of which *E. coli* is the most common potential pathogen. During the progression of liver fibrosis to cirrhosis, the number of *Enterobacteriaceae* bacteria in the body increases dramatically. This increase leads to the release of large amounts of endotoxin in the plasma, which in turn inhibits the synthesis of intestinal epithelial proteins and impairs intestinal barrier function. This triggers a series of complex pathological effects, such as bacterial translocation, which ultimately leads to an imbalance in the structure of the intestinal flora [38].

The theory that the liver is connected to the large intestine was first mentioned in Chinese medicine in the Treatise on the Interpolation of the Five Organs [39], which is similar to the theory of the gut–liver axis in modern medicine. The physiological coordination, pathology, mutual influence, turbid obstacles, and turbid gas in the liver and large intestine increase, followed by the loss of excretion in the liver. Conversely, if the liver stagnates, the loss of regulation in the liver and can affect the opening and closing of the turbid discharge in the large intestine. Patients with WD often experience innate deficiencies, copper toxicity, and impaired excretion. Over time, copper accumulates in the liver and contributes to dampness, heat, phlegm, and blood stasis. These conditions can lead to symptoms such as shaking limbs, writhing of hands and feet, and tonic contractures, which are observable in affected patients. As the course of the disease lengthens, tangible real evils further gather, the positive qi weakens, the pattern of evidence changes from solid to deficient, and the condition is further aggravated [40]. A previous study reported [41] that spleen and kidney yang deficiency was the most serious type of WD-related liver injury, and our present study also revealed that patients with spleen and kidney yang deficiency presented the most significant decrease in the abundance of the intestinal flora. Moreover, the decrease in the content of probiotics and the increase in the content of potentially pathogenic bacteria were extremely significant. In addition, there were significant differences in the structure and composition of the intestinal flora between patients in the A, B, and C solid evidence groups and patients in the D and E deficiency evidence groups. The above results can provide new insights into the dialectical typing of patients with WD-related liver fibrosis and the development of individualized diagnostic and treatment strategies.

In this study, we investigated the diversity and variability of the intestinal flora in patients with different evidence of WD-related liver fibrosis to further analyze and explore the possible underlying causes. During the evolution of WD patients from the damp-heat internalization, phlegm-blood stasis mutualization, and liver-wind internalization to liver-kidney deficiency and spleen-kidney yang deficiency patterns, the level of liver inflammation and fibrosis also continues to progress, and the composition of

doi: 10.12938/bmfh.2024-081

the intestinal flora undergoes dynamic and significant changes. The external manifestations of different types of symptoms are closely related to the internal flora structure, which is also in line with the basic characteristics of the "holistic view" of the Chinese medicine theory system. This study provides evidence from Chinese medicine for the treatment of WD-related liver fibrosis, which provides a theoretical basis and new ideas for the differential diagnosis, prevention, and treatment of this disease in Chinese medicine.

However, there are still some shortcomings in this study. First, the sample size of this study is small and the results are not representative and generalizable. In the future, we need to expand the sample size to further explore the differences between the intestinal flora of WD patients. Second, our study illustrated only the correlation between intestinal flora and different syndromes in WD-related liver fibrosis patients, but we did not study the underlying mechanisms in depth. Therefore, it is still necessary to systematically study the specific pathogenic mechanisms that cause changes in the intestinal flora across different syndromes to provide new breakthroughs in the field of traditional Chinese medicine for WD-related liver fibrosis.

AUTHOR'S CONTRIBUTION

Conception and design: J Zhang, H Wang, and Y Pu. Administrative support: J Zhang and D Xie. Provision of study materials or patients: Y Ma and H Chen. Collection and assembly of data: R Li and H Ye. Data analysis and interpretation: Y Pu, N Peng, and R Li. Manuscript writing: All authors. Final approval of manuscript: All authors.

DATA AVAILABILITY

Data are available through reasonable request to the corresponding author.

FUNDING

This work was supported by the National Natural Science Foundation of China (Grant No. 82274493), the National Natural Science Foundation of China (Grant No. 81774299), the Scientific Research Program of Universities in Anhui Province (Grant No. 2023AH050791), and the Scientific Research Program of the Chinese Society of Ethnomedicine (No. 2020ZY070-410033).

CONFLICT OF INTEREST

The authors declare that they have no known competing financial interests or personal relationships that could have appeared to influence the work reported in this paper.

REFRENCES

1. Cheng C, Wang Q, Huang Y, Xue Q, Wang Y, Wu P, Liao F, Miao C. 2023. Gandouling inhibits hepatic fibrosis in Wilson's disease through Wnt-1/β-catenin signaling pathway. J Ethnopharmacol 311: 116445. [Medline] [CrossRef]
2. Zhang J, Xiao L, Yang W. 2020. Combined sodium Dimercaptopropanesulfonate and zinc versus D-penicillamine as first-line therapy for neurological Wilson's disease. BMC Neurol 20: 255. [Medline] [CrossRef]
3. Tang L, Zhao C, Zhang J, Dong T, Chen H, Wei T, Wang J, Yang W. 2023. Discussion on the mechanism of gandoufumu decoction attenuates liver damage of Wilson's disease by inhibiting autophagy through the PI3K/Akt/mTOR pathway based on network pharmacology and experimental verification. Mediators Inflamm 2023: 3236911. [Medline] [CrossRef]
4. Iwański S, Seniów J, Leśniak M, Litwin T, Członkowska A. 2015. Diverse attention deficits in patients with neurologically symptomatic and asymptomatic Wilson's disease. Neuropsychology 29: 25–30. [Medline] [CrossRef]
5. Gerosa C, Fanni D, Congiu T, Piras M, Cau F, Moi M, Faa G. 2019. Liver pathology in Wilson's disease: from copper overload to cirrhosis. J Inorg Biochem 193: 106–111. [Medline] [CrossRef]
6. Bandmann O, Weiss KH, Kaler SG. 2015. Wilson's disease and other neurological copper disorders. Lancet Neurol 14: 103–113. [Medline] [CrossRef]
7. Xia S, Huang Y, Zhang Y, Zhang M, Zhao K, Han P, Tian D, Liao J, Liu J. 2023. Role of macrophage-to-myofibroblast transition in chronic liver injury and liver fibrosis. Eur J Med Res 28: 502. [Medline] [CrossRef]
8. Zhang W, Shao M, Zhang H, Wu Z, Miao T, Zheng H, Xie X, Wang R. 2018. Study on the regulation of miR-122 gene related factors expression in liver fibrosis by Fuzheng Huayu tablets. J Beijing Univ Traditional Chinese Med 41: 76–82 (in Chinese).
9. Lu WM, Yan LX, Ye JS, Du J, Zhou L. 2024. Progress of mesenchymal stem cell exosomes in the treatment of liver fibrosis. JiangXi Medical Journal 59: 509–513 (Chinese).
10. Zhang Z, Yuan Y, Hu L, Tang J, Meng Z, Dai L, Gao Y, Ma S, Wang X, Yuan Y, *et al.* 2023. ANGPTL8 accelerates liver fibrosis mediated by HFD-induced inflammatory activity via LILRB2/ERK signaling pathways. J Adv Res 47: 41–56. [Medline] [CrossRef]
11. Wang N, Wu W, Wen B, Deng X. 2024. Research progress of traditional Chinese medicine and hepaticfibrosis based on the theory of "gut-liver axis". J Shanxi Univ Traditional Chinese Med 25: 109–112, 118 (in Chinese).
12. Collins SL, Stine JG, Bisanz JE, Okafor CD, Patterson AD. 2023. Bile acids and the gut microbiota: metabolic interactions and impacts on disease. Nat Rev Microbiol 21: 236–247. [Medline] [CrossRef]
13. Chávez-Talavera O, Tailleux A, Lefebvre P, Staels B. 2017. Bile acid control of metabolism and inflammation in obesity, type 2 diabetes, dyslipidemia, and nonalcoholic fatty liver disease. Gastroenterology 152: 1679–1694.e3. [Medline] [CrossRef]
14. Xie G, Wang X, Huang F, Zhao A, Chen W, Yan J, Zhang Y, Lei S, Ge K, Zheng X, *et al.* 2016. Dysregulated hepatic bile acids collaboratively promote liver carcinogenesis. Int J Cancer 139: 1764–1775. [Medline] [CrossRef]
15. Zhang HL, Yu LX, Yang W, Tang L, Lin Y, Wu H, Zhai B, Tan YX, Shan L, Liu Q, *et al.* 2012. Profound impact of gut homeostasis on chemically-induced pro-tumorigenic inflammation and hepatocarcinogenesis in rats. J Hepatol 57: 803–812. [Medline] [CrossRef]
16. Socała K, Doboszewska U, Szopa A, Serefko A, Włodarczyk M, Zielińska A, Poleszak E, Fichna J, Wlaź P. 2021. The role of microbiota-gut-brain axis in neuropsychiatric and neurological disorders. Pharmacol Res 172: 105840. [Medline] [CrossRef]
17. Guan H, Zhang X, Kuang M, Yu J. 2022. The gut-liver axis in immune remodeling of hepatic cirrhosis. Front Immunol 13: 946628. [Medline] [CrossRef]
18. Milosevic I, Vujovic A, Barac A, Djelic M, Korac M, Radovanovic Spurnic A, Gmizic I, Stevanovic O, Djordjevic V, Lekic N, *et al.* 2019. Gut-liver axis, gut microbiota, and its modulation in the management of liver diseases: a review of the literature. Int J Mol Sci 20: 395. [Medline] [CrossRef]
19. Wang L, Cao ZM, Zhang LL, Li JM, Lv WL. 2022. The role of gut microbiota in some liver diseases: from an immunological perspective. Front Immunol 13: 923599. [Medline] [CrossRef]
20. Lee NY, Suk KT. 2020. The role of the gut microbiome in liver cirrhosis treatment. Int J Mol Sci 22: 199. [Medline] [CrossRef]
21. Zhang YL, Li ZJ, Gou HZ, Song XJ, Zhang L. 2022. The gut microbiota-bile acid axis: a potential therapeutic target for liver fibrosis. Front Cell Infect Microbiol 12: 945368. [Medline] [CrossRef]
22. Wei TH, Qian NN, Yang WM, Xie DJ, Bao YC, Tong JB, Hao WJ, Yang Y. 2022. Exploring the clinical characteristics of liver fibrosis in Wilson's disease of different Chinese medicine certificates based on liver stiffness value combined with multidimensional indexes. Chinese J Integrative Med Cardio-/Cerebrovascuiar Disease 20: 2738-2742 (in Chinese).
23. Dong W, Hao WJ, Yang WM, Huang P. 2023. Study on the correlation between the degree of hepatic fibrosis and Chinese medicine evidence in hepatoblastic nuclear degeneration. J Anhui Univ Chinese Med 42: 19–23 (Chinese).
24. Neurogenetics Group, Neurology Branch, Chinese Medical Association. 2021. Chinese guidelines for the diagnosis and treatment of hepatolenticular degeneration 2021. Chin J Neurol 54: 310–319 (in Chinese).
25. Xu L, Liu P, Shen X, Wu Y, Ping J. 2019. Guidelines for the diagnosis and treatment of liver fibrosis by combining traditional chinese and western medicine (2019 edition). Chinese J Integrated Traditional Western Med 39: 1286–1295 (in Chinese).
26. Neurogenetics Group of the Neurology Section of the Chinese Medical Association. 2021. Guidelines for the diagnosis and treatment of hepatomegaly in China 2021. Chin J Neurol 54: 310–319 (in Chinese).
27. Liu YT, Qi SL, Sun KW. 2021. Traditional Chinese medicine, liver fibrosis, intestinal flora: is there any connection?—a narrative review. Ann Palliat Med 10: 4846–4857. [Medline] [CrossRef]

28. Albhaisi SAM, Bajaj JS, Sanyal AJ. 2020. Role of gut microbiota in liver disease. Am J Physiol Gastrointest Liver Physiol 318: G84–G98. [Medline] [CrossRef]
29. Pushpanathan P, Mathew GS, Selvarajan S, Seshadri KG, Srikanth P. 2019. Gut microbiota and its mysteries. Indian J Med Microbiol 37: 268–277. [Medline] [CrossRef]
30. Chen T, Ding R, Chen X, Lu Y, Shi J, Lü Y, Tang B, Zhang W, Ye C, Yuan M, *et al.* 2021. *Firmicutes* and *Blautia* in gut microbiota lessened in chronic liver diseases and hepatocellular carcinoma patients: a pilot study. Bioengineered 12: 8233–8246. [Medline] [CrossRef]
31. Seong CN, Kang JW, Lee JH, Seo SY, Woo JJ, Park C, Bae KS, Kim MS. 2018. Taxonomic hierarchy of the phylum Firmicutes and novel Firmicutes species originated from various environments in Korea. J Microbiol 56: 1–10. [Medline] [CrossRef]
32. Binda C, Lopetuso LR, Rizzatti G, Gibiino G, Cennamo V, Gasbarrini A. 2018. Actinobacteria: a relevant minority for the maintenance of gut homeostasis. Dig Liver Dis 50: 421–428. [Medline] [CrossRef]
33. Usami M, Miyoshi M, Yamashita H. 2015. Gut microbiota and host metabolism in liver cirrhosis. World J Gastroenterol 21: 11597–11608. [Medline] [CrossRef]
34. Ashour Z, Shahin R, Ali-Eldin Z, El-Shayeb M, El-Tayeb T, Bakr S. 2022. Potential impact of gut *Lactobacillus acidophilus* and *Bifidobacterium bifidum* on hepatic histopathological changes in non-cirrhotic hepatitis C virus patients with different viral load. Gut Pathog 14: 25. [Medline] [CrossRef]
35. Corthésy B, Gaskins HR, Mercenier A. 2007. Cross-talk between probiotic bacteria and the host immune system. J Nutr 137 Suppl 2: 781S–790S. [Medline] [CrossRef]
36. Xue L, He J, Gao N, Lu X, Li M, Wu X, Liu Z, Jin Y, Liu J, Xu J, *et al.* 2017. Probiotics may delay the progression of nonalcoholic fatty liver disease by restoring the gut microbiota structure and improving intestinal endotoxemia. Sci Rep 7: 45176. [Medline] [CrossRef]
37. Cuesta S, Burdisso P, Segev A, Kourrich S, Sperandio V. 2022. Gut colonization by Proteobacteria alters host metabolism and modulates cocaine neurobehavioral responses. Cell Host Microbe 30: 1615–1629.e5. [Medline] [CrossRef]
38. Mou H, Yang F, Zhou J, Bao C. 2018. Correlation of liver function with intestinal flora, vitamin deficiency and IL-17A in patients with liver cirrhosis. Exp Ther Med 16: 4082–4088. [Medline]
39. Wang C, Ji Y. 2021. Preliminary study and application of the theory of "connection between the liver and the large intestine". J Zhejiang Chinese Med Univ 45: 339–344 (in Chinese).
40. Szabo G, Bala S, Petrasek J, Gattu A. 2010. Gut-liver axis and sensing microbes. Dig Dis 28: 737–744. [Medline] [CrossRef]
41. Huang P, Dong T, Li X, Wang H, Wang MX, Yang WM. 2022. Comparison the changes of related indexes of different traditional Chinese medicine syndrome types in patients with hepatolenticular degeneration. China Medical Herald 19: 163–166 (in Chinese).

doi: 10.12938/bmfh.2024-081